Biosorption of praseodymium (III) using *Terminalia arjuna* bark powder in batch systems: isotherm and kinetic studies

Krishna Kumari Swain, Pravat Manjari Mishra and Aparna Prabha Devi

ABSTRACT

The high demand for rare earth elements (REEs) used in various advanced materials implies demand for increased production of REEs or the recycling of solutions to recover the REEs they contain. In this study, the biosorption of Pr(III) from aqueous solution by bark powder of *Terminalia arjuna* was examined in a batch system as a function of metal concentration, biosorbent dosage, pH and contact time. Results showed that *T. arjuna* bark powder has a high affinity for adsorbing Pr(III): more than 90% at pH 6.63. The adsorption of Pr(III) by *T. arjuna* bark powder was investigated by the Langmuir, Freundlich, Temkin and Dubinin-Radushkevich isotherm models. The kinetics of the biosorption process was tested with pseudo-first-order and pseudo-second-order models, and the results showed that the biosorption process was better fitted to the pseudo-second-order model. From Fourier transform infrared spectroscopy (FT-IR) analysis, it is confirmed that the biomolecules of *T. arjuna* bark powder are involved in the biosorption process of Pr(III) metal ions.

Key words | adsorption, isotherms, kinetics, praseodymium, rare earth metal, *Terminalia arjuna*

Krishna Kumari Swain
Pravat Manjari Mishra (corresponding author)
Aparna Prabha Devi
Environment & Sustainability Department,
CSIR-Institute of Minerals and Materials Technology,
Bhubaneswar, Odisha 751013,
India
E-mail: *pravatmanjari@yahoo.co.in*; *pravatmanjari@immt.res.in*

INTRODUCTION

In the past few years, researchers across the world have shown increasing interest in the rare earth elements (REEs), due to their unique properties and their applications in defence, metallurgy, ceramic industries, and chemical industries (Das & Das 2013; Zhu *et al.* 2015). They are also used in making high-level superconductors and ultraviolet absorbers, cracking catalysts for petroleum, illuminators, electronics, miniaturized equipment, secondary batteries, satellites, etc. (Das & Das 2013), and also in the fields of medicine and agriculture. REEs in the periodic table are generally thought of as the 17 elements which include scandium (Sc), yttrium (Y), and the lanthanides. One of the lanthanide elements, praseodymium (Pr), is a strategic material which is employed for making powerful and permanent magnets, hydrogen storage materials, battery materials and glass materials, etc. (Zhang *et al.* 2014). That is why its recovery from waste is very important.

REEs are profusely available in nature, but their separation and purification is very complex and expensive. The predominant methods that are used for the recovery of REEs are chemical precipitation, ion exchange, solvent extraction, electrochemical separation, and flocculation, etc. involving the use of toxic chemicals which are very harmful to the environment. Thus, there is a great need to develop a cost-effective and eco-friendly method to separate out REEs.

The most cost-effective, eco-friendly and innovative technology for separation of REEs is biosorption. Biosorption is a process in which uptake of metal or metalloid particulates through adsorption is done by biological species. Because of their versatility, effectiveness and abundant availability, as well as the fact that they are safe to handle and free from toxic chemicals, biosorbents are widely used. Biomass contains various functional groups such as carboxylates, phenolics, esters, amides, phosphates, and carbonyl and sulfhydryl groups in the form of polysaccharides, lignin, proteins, and other polymers which are found in the cells or cell walls.

Some researchers have studied the recovery of REEs by different biosorbents such as cerium (Ce) biosorption by corn styles and prawn carapaces (Varsihini *et al.* 2014), erbium (Er) and holmium (Ho) biosorption by modified alfalfa biomass (Gardea-Torresdey *et al.* 2004), biosorption of REEs by salmon milt (Takahashi *et al.* 2014), recovery of lanthanum (La) by fish scale and neem sawdust (Das *et al.* 2014),

doi: 10.2166/wst.2017.589

biosorption of lutetium (Lu) by herbal plant samples (Soylak & Murat 2014). Recently, Anastopoulos *et al.* have carried out a literature review regarding the removal of rare earth metals from aqueous solutions by different low-cost adsorbents (Anastopoulos *et al.* 2016). But to date very little literature is available on the separation or recovery of REEs by biosorbents, and the work on the recovery of Pr metal by biosorption is negligible. Oliveira *et al.* studied the biosorption of Pr using *Sargassum* sp. (Oliveira *et al.* 2011). Philip *et al.* studied the biosorption of Pr using *Pseudomonas aeruginosa* (Philip *et al.* 2000). Vijayaraghavan studied the biosorption of Pr using *Ulva lactuca*, a green seaweed (Vijayaraghavan 2015).

In this study we have for the first time used the powdered bark of *Terminalia arjuna*, rich in polyphenolic compounds, to study the adsorption of Pr metal. *T. arjuna* is a large, evergreen tree belonging to the Combretaceae family. Biosorption mainly involves the metal binding with biomolecules containing polar functional groups such hydroxyl and carboxyl groups, etc. Since arjunic acid, terminic acid, glycosides, flavones, flavonoids, tannins, oligomeric proanthocyanidins and minerals are present in the bark of *T. arjuna* (Nema *et al.* 2012), we selected this plant for a biosorption study of Pr in a batch system. The study was divided into five parts: (a) the effect of different process parameters on adsorption of Pr metal by *T. arjuna* bark powder was studied and was optimized to achieve the maximum adsorption of Pr(III); (b) characterization of the biomass before and after the metal adsorption; (c) determination of biosorption isotherms; (d) equilibrium and kinetic studies of biosorption; (e) regeneration of the biosorbent.

MATERIALS AND METHODS

Biomass collection

The bark of *T. arjuna* plant was collected in Bhadrak district, Odisha, India on a sunny day. The collected samples were washed thoroughly to remove the dust and other particles. The washed samples were then put into a hot-air oven at 60 °C for 3–4 days. The oven-dried samples were ground to a fine powder and then sieved to 63 mesh. Afterwards it was stored in a plastic bottle for future use.

The stock solution of Pr (1,000 mg/L) was prepared by dissolving 1.170 g of Pr_2O_3 (Merck Pvt. Ltd) in 1,000 mL of deionized water. The variations of concentration were done by diluting the stock solution as required for the experiment. Sodium hydroxide NaOH 0.01 N (Rankem) and sulphuric acid H_2SO_4 0.01 M (Qualigens) were used for pH adjustment.

Batch experiments

The batch adsorption experiment was carried out in a 100 mL capped conical flask containing 20 mL of Pr(III) metal solution rotated at 200 rpm, at room temperature (28 °C) for 8 hours. In the present study the initial metal concentration (10–80 mg/L), adsorbent dose (0.01–0.1 g), pH (1.0–11.0) were used to obtain the optimum conditions for metal adsorption. To maintain the pH of the solution 10% H_2SO_4 and 0.1 M NaOH were used. The samples were taken out at different time intervals. The solid residues were separated from the solution by the centrifuge method after equilibrium was reached. The filtrate was analyzed under UV-Visible spectroscopy (JASCO, V-650 model) at maximum wavelength 655 nm to analyze the residual metal concentration. All the experiments were carried out at least three times. The percentage removal of Pr(III) E and the amount of metal uptake Q were determined as below.

$$\%\mathrm{E} = \left(\frac{C_i - C_f}{C_i}\right) \times 100$$

where, C_i is the initial Pr(III) metal concentration (mg/L), C_f is the equilibrium concentration of Pr(III) metal solution.

$$\mathrm{Q} = \left(\frac{C_i - C_f}{\mathrm{M}}\right) \times \mathrm{V}$$

where M is the amount of dry biomass (g) used for biosorption and V is the volume of the metal solution (L).

Equilibrium isotherms and kinetic studies

In this study the equilibrium data were analyzed by using four isotherm models, i.e. Langmuir, Freundlich, Temkin and Dubinin–Radushkevich. The kinetics of adsorption was based on the contact time required to reach equilibrium. The experiments were carried out at optimized conditions and withdrawals of samples were done at regular intervals (30–1,200 min). The data of the experiment were analyzed by pseudo-first-order and pseudo-second-order kinetics models respectively.

Scanning electron microscopic analysis

The surface morphology of *T. arjuna* bark powder before and after adsorption was studied by scanning electron microscopy (SEM; JEOL, JSM-6510).

Fourier transform infrared spectroscopy analysis

Fourier transform infrared spectroscopy (FT-IR) was used to identify the functional groups that were present in the *T. arjuna* bark powder before and after adsorption of metal. The IR spectra were reported on a FT-IR spectrometer (ALPHA, BRUKER) using the KBr disc method. For this experiment, 5 mg of adsorbent was used. The wavelength of transmission spectra varies from 500 cm^{-1} to 4,000 cm^{-1} with a resolution of 4 cm^{-1}.

Energy dispersive X-ray analysis

The energy dispersive X-ray (EDAX) analysis before and after adsorption was conducted using Tecnai G220 Twin, D2044 (FEI Co., Eindhoven, The Netherlands). The voltage was maintained at 20 kV.

Regeneration study of biomass

In the regeneration study, the *T. arjuna* bark powder was tested for the removal and recovery of praseodymium. The adsorption experiment was carried out for 8 hours at a concentration of 80 mg/L and 0.09 g of biomass. The sample was centrifuged and the supernatant was tested for metal analysis. The Pr(III)-loaded *T. arjuna* bark powder was subjected to 0.1 mol/L HCl and was rinsed twice in deionized water. The regenerated biosorbent was used in the next adsorption cycle and again regenerated and used for the removal of Pr(III) at different concentrations in the range of 20–80 ppm. The process was continued till the adsorption capacity of adsorbent shows its lowest adsorption capacity.

RESULTS AND DISCUSSION

Influence of initial metal concentration

The biosorption capacity of the *T. arjuna* bark powder for Pr metal extraction increased with increasing concentration of Pr. The adsorption percentage increased from 51% to 91%, with the increase in metal concentration from 10 mg/L to 80 mg/L but after that no significant change in adsorption percentage was observed, as shown in Figure 1(a). This was because the concentration of bisorbent was fixed, and so the total available adsorption sites were limited. After equilibrium, due to the non-availability of adsorption sites on the adsorbent, there was decrease in the percentage removal of the adsorbate corresponding to an increase in initial metal concentration. Similar results were found by Awwad *et al.* in 2010 (Awwad *et al.* 2010). The results showed that the removal of Pr(III) was concentration dependent.

Influence of adsorbent dose

At a fixed metal concentration, with an increase in biosorbent dosage, the adsorption percentage increased to a certain level, then decreased. At the equilibrium time of 8 hours, the adsorption percentage increased from 41.98% to 91.71%, when the biomass concentration was increased from 0.01 g/L to 0.09 g/L (Figure 1(b)). This might have been due to the fact that, with an increase in biomass concentration, there was an increase in the surface area of the biosorbent which ultimately increased the number of adsorption sites (Esposito *et al.* 2001). A further increase in the biomass concentration over 0.09 g/L did not bring about a significant improvement in biosorption at the adsorption equilibrium, due to saturation of the adsorbate with the adsorbent, since the concentration of adsorbate was fixed. These results suggest that the dosage of a biosorbent strongly influences the extent of biosorption.

Influence of pH on adsorption

Biosorption is strongly controlled by pH, which affects the speciation of metals in solution through hydrolysis, complexation and redox reactions during metal recovery (Kazy *et al.* 2006; Qing 2010). In this study, the adsorption percentage increased from 91.47 to 94.15% (Figure 1(c)) when the initial solution pH increased from 1.91 to 6.63. The adsorption capacity decreased at low pH values due to the increase in concentration of H^+ ions, which competed with the Pr(III) metal ions for the same binding sites on the biosorbent; there was a decrease in the metal's biosorption potential due to the increased positive charge density on the binding sites. At a higher pH, the functional groups of the biosorbent are deprotonated, which leads to an increase in sorptive capacity for metal ions (Anastopoulos *et al.* 2013). Similar results were obtained in the case of adsorption of La(III) and Ce(III) using A*grobacterium* sp. HN1 when the pH was increased to 6.8 (Xu *et al.* 2011). But there was decrease in adsorption percentage from 94.16 to 89.58% when the pH was further increased from 6.63 to 11.81. This might have been due to the hydrolysis of the metal ion with the formation of the corresponding insoluble hydroxide due to the presence of excess of OH^- ions at the higher pH.

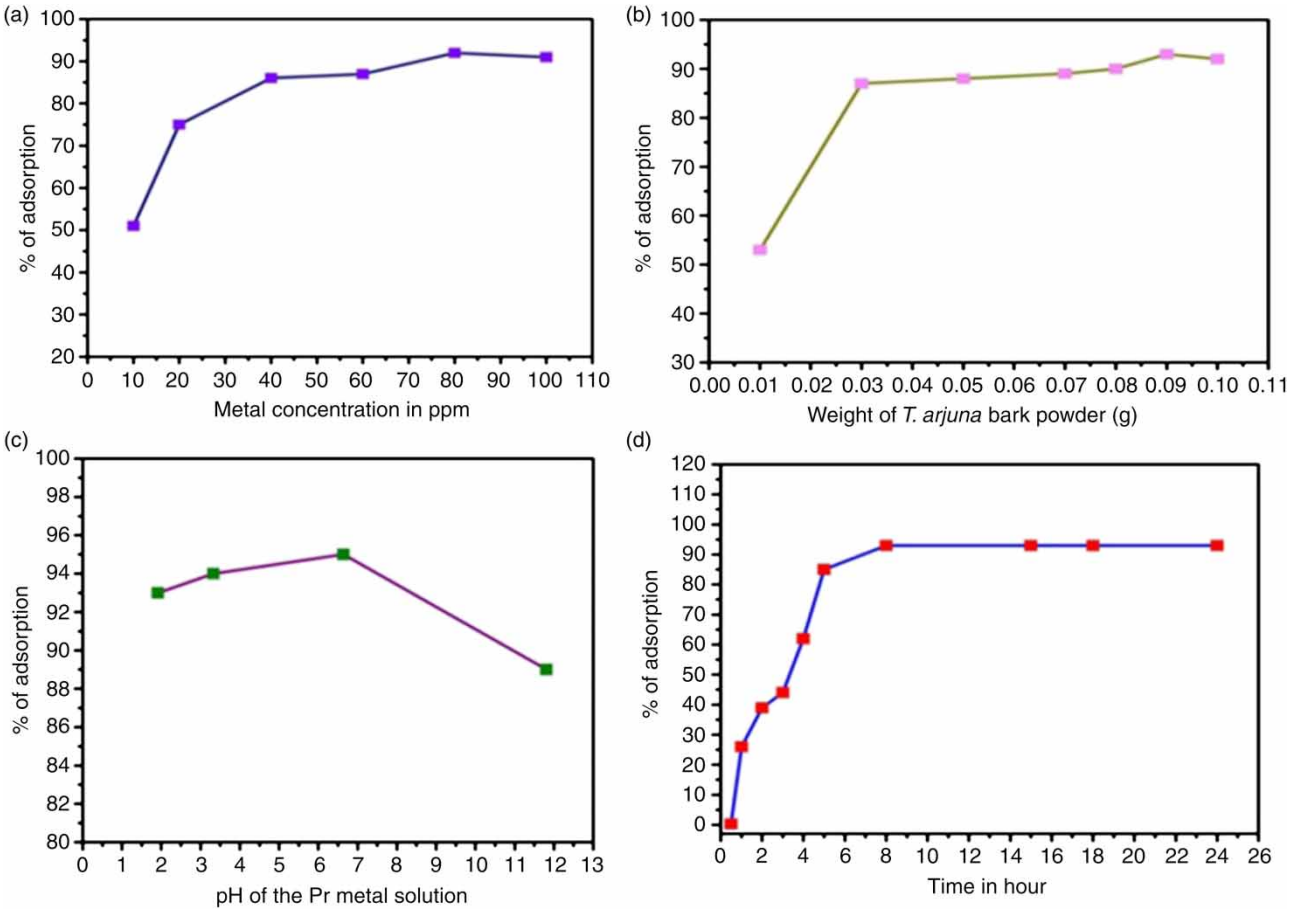

Figure 1 | (a) Effect of metal concentration: rotation = 200 rpm, W = 0.1 g, V = 20 mL, T = 298.13 K, and pH = 2.5 ± 0.05; (b) effect of adsorbent dose: rotation = 200 rpm, W = 0.1 g, Ci = 80 ppm, V = 20 mL, T = 298.13 K, and pH = 2.5 ± 0.05; (c) effect of pH: rotation = 200 rpm, W = 0.1 g, C_i = 80 ppm, V = 20 mL and T = 298.13 K.; (d) effect of contact time: rotation = 200 rpm, W = 0.1 g, C_i = 80 ppm, V = 20 mL and T = 298.13 K.

Influence of contact time on adsorption

Contact time is an important parameter which affects the adsorption capacity of an adsorbent (Kütahyali *et al.* 2010; Vijayaraghavan *et al.* 2010). With the increase in contact time from 20 min to 8 hours the adsorption percentage increased and thereafter the adsorption rate remained constant (Figure 1(d)). This might have been due to the instantaneous utilization of the most readily available active sites on the surface of the biosorbent. After a period of contact time the biosorption remained the same due to the unavailability of binding sites on the adsorbent surface. Therefore, this contact time could be taken as equivalent to the equilibrium time. Similar results were obtained by Qing in 2010 (Qing 2010). He reported that the adsorption capacity of La(III) increased with the increase in contact time up to 480 min for modified bamboo charcoal, after which no significant increase in La(III) adsorption occurred.

Adsorption isotherm studies

An inspection of the mechanism of the adsorption process and the relationship between adsorbate and adsorbent was carried out using four models: the Langmuir, Freundlich, Temkin and Dubinin–Radushkevich isotherm models. The values of the isotherm constants for the four models were obtained and are presented in Table 1.

Langmuir adsorption isotherm

The Langmuir adsorption isotherm (Langmuir 1916) generally explains the monolayer adsorption of an adsorbate on the outer surface of the adsorbent having a finite number of identical sites, after which further adsorption does not takes place (Foo & Hammed 2010). This isotherm describes the equilibrium distribution of metal ions between the solid and liquid phases. It further establishes the uniform energies of adsorption onto the surface of adsorbent, and

Table 1 | Langmuir, Freundlich, Temkin and Dubinin–Radushkevich isotherm constants for the sorption of Pr(III) on *T. arjuna* bark powder

Langmuir isotherm				**Freundlich isotherm**			
R^2	Q_{max} (mg/g)	b (L/mg)	R_L	R^2	K_f (mg/g)(L/mg)$^{1/n}$	n	1/n
0.986	1.22	0.187	0.35	0.954	10.49	0.377	2.65
Temkin isotherm				**Dubinin–Radushkevich isotherm**			
R^2	B (J/mol)	b_t (J/mol)	At (L/g)	R^2	E (kg/mol)	B (mg/g)	Q_{max}
0.97	34.64	72.72	2.837	0.98	0.002	83453	24.21

transmigration of adsorbate does not take place in the plane of the surface. The equation of the Langmuir isotherm model is given below.

$$\frac{C_e}{Q_e} = \frac{1}{b*Q_{max}} + \frac{C_e}{Q_{max}}$$

C_i = initial concentration (mg/L)
$Q_e = \frac{[(C_i - C_e)*\mathrm{v}]}{w}$ = adsorption capacity (mg/g)
C_e = equilibrium concentration (mg/L)
v = volume taken for adsorption study (L)
w = weight of sample taken for adsorption study (g)
b = Langmuir isotherm constant (L/mg)

The values of Q_{max} and b were computed from the slope and intercept of the Langmuir plot of C_e versus C_e/Q_e. The essential features of the Langmuir isotherm may be expressed in terms of the separation factor R_L which is calculated by using the equation given below.

$$R_L = \frac{1}{1 + b*C_i}$$

The R_L value indicates the adsorption nature to be either unfavourable if $R_L > 1$, linear if $R_L = 1$, favourable if $0 < R_L < 1$ and irreversible if $R_L = 0$.

From this research work, in the case of sorption of Pr(III) onto *T. arjuna* bark powder, the maximum monolayer coverage capacity (Q_{max}) from the Langmuir isotherm model (Figure 2(a)) was determined to be 1.225 mg/g, b (the Langmuir isotherm constant) is 0.187 L/mg, R_L (the separation factor) is 0.35 (Table 1), indicating that the equilibrium sorption was favourable. The R^2 value was 0.986, proving that the sorption data fitted the Langmuir isotherm model well.

Freundlich adsorption isotherm

The Freundlich isotherm is literally meant for heterogeneous surface involving multi layer adsorption (Foo & Hammed 2010). This isotherm is an empirical relationship between the concentration of a solute on the surface of an adsorbent and the concentration of the solute in the liquid with which it is in contact. The equation of the Freundlich adsorption isotherm is given below.

$$\log Q_e = \log K_f + \frac{1}{n}\log C_e$$

K_f = an approximate indicator of adsorption capacity (mg/g) (L/mg)$^{1/n}$
1/n = a function of the strength of adsorption in the adsorption process
C_e = equilibrium concentration (mg/L)

The values of C_e, Q_e and n were obtained from the intercept and slope of a graph log Q_e vs. log C_e. The adsorption isotherm depends on both the parameters K_f and n. The adsorption capacity varies with the values of K_f and n, i.e. greater values of n and K_f, are more favorable for adsorption. If n = 1 then the partition between the two phases is independent of the concentration. If the value of 1/n is below 1 it indicates a normal adsorption. On the other hand, 1/n being above 1 indicates cooperative adsorption. Therefore n should lie in between 2 and 10.

In the present study, from the Freundlich isotherm model of sorption of Pr(III) onto *T. arjuna* bark powder (Figure 2(b)), the value of 1/n is found to be 2.65 and the value of n is 0.377 (Table 1), which indicates that the sorption is unfavourable.

Temkin adsorption isotherm

The Temkin isotherm describes that due to adsorbent-adsorbate interaction, the heat of adsorption of all the molecules in the layer decreases linearly and the adsorption is characterized by a uniform distribution of binding energies. The Temkin isotherm is represented by the following equations (Temkin & Pyzhev 1940).

$$Q_e = \frac{RT}{b_t}\ln A_t + \frac{RT}{b_t}\ln C_e$$

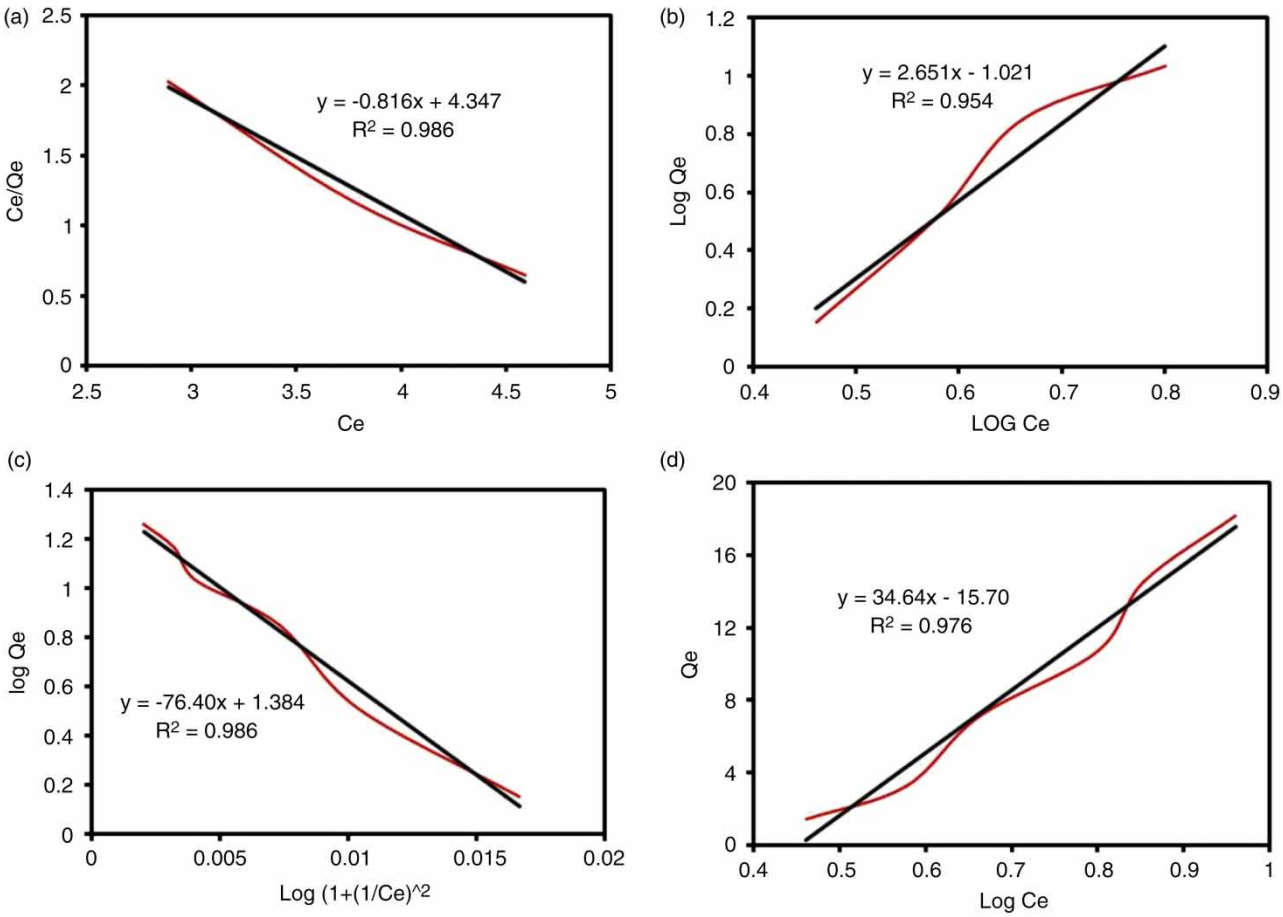

Figure 2 | (a) Langmuir adsorption isotherm for the sorption of Pr(III) on *T. arjuna* bark powder; (b) Freundlich adsorption isotherm for the sorption of Pr(III) on *T. arjuna* bark powder; (c) Temkin adsorption isotherm for the sorption of Pr(III) on *T. arjuna* bark powder; (d) Dubinin–Radushkevich Isotherm for the sorption of Pr(III) on *T. arjuna* bark powder.

$$\frac{RT}{b_t} = B$$

A_t = Temkin isotherm equilibrium binding constant (L/mg)
b_t = Temkin isotherm constant (J/mol)
R = universal gas constant (8.314 J/mol/K)
T = temperature at 298 K
B = constant related to heat of adsorption (J/mol)

In case of sorption of Pr(III) on *T. arjuna* bark powder, the values obtained by this model (Figure 2(c)) were as follows: the Temkin constant (b_t) were 72.72 J/mol and equilibrium binding constant was 34.64 L/mg, which were an indication of the heat of sorption, indicating a physical adsorption process; $R^2 = 0.976$ (Dada *et al.* 2012).

Dubinin–Radushkevich isotherm model

The Dubinin–Radushkevich isotherm is mainly used to describe the mechanism of adsorption of subcritical vapours onto a heterogeneous surface (Dubinin & Radushkevich 1947; Dabrowski 2001). The linear form of the equation is:

$$\log Q_e = \log Q_{max} - \frac{1}{2E^2} * \left[RT \log\left(1 + \frac{1}{C_e}\right)\right]^2$$

$$\text{Slope} = -B * R^2 * T^2$$

$$E = \frac{1}{\sqrt{2B}}$$

Q_e = equilibrium adsorption capacity (mg/g)
C_e = equilibrium final concentration (mol/L)
R = ideal gas constant (8.314 J/mol K)
T = absolute temperature (303 K)
$E = RT \log (1 + 1/C_e)$ (kJ/mol)

If E value lies between 8 and 16 kJ/mol then it is said to be chemosorption, and values below 8 kJ/mol show physical adsorption.

In case of sorption of Pr(III) on *T. arjuna* bark powder, from the linear plot of the Dubinin–Radushkevich model

(Figure 2(d)), Q_e was determined to be 24.21 mg/g, the mean free energy, $E = 0.002$ kJ/mol indicating a physiosorption process; $R^2 = 0.986$.

Adsorption kinetics studies

In order to find the information on the kinetics of adsorption of Pr(III) metal ions by *T. arjuna* bark powder, two kinetic parameters were used: the pseudo-first-order and pseudo-second-order kinetics models.

The pseudo-first-order equation (Langergren & Svenska 1898) was used to determine the rate constant of the adsorption process:

$$\log (Q_e - Q_t) = \log Q_e - K_1 t$$

where, Q_e = the amount of solute adsorbed on the surface at equilibrium (mg/g), Q_t = the amount of solute adsorbed at time t (mg/g), K_1 = the rate constant (h^{-1}), t = time interval (hours).

The pseudo-second-order equation can be expressed in linear form as:

$$\frac{t}{Q_t} = \frac{1}{K_2 Q_e^2} + \frac{1}{Q_e} t$$

where, t = the time interval taken in hours, K_2 = the rate constant (g mg^{-1} h^{-1}), Q_t = the amount of solute adsorbed at time t (mg/g).

The models were examined by linear plots of log (Q_e–Q_t) versus t (Figure 3(a)) and (t/Q_t) versus t (Figure 3(b)). The models' characteristic parameters and regression co-efficients are listed in Table 2. In the case of the pseudo-first-order kinetic model, the value of R^2 is low i.e. 0.7919 and the experimental Q_e value does not agree well with the calculated Q_e value. This shows that the adsorption of Pr(III) onto *T. arjuna* bark powder is not first-order kinetics. But the pseudo-second-order model yielded a high correlation coefficient ($R^2 > 0.97$) and the experimental Q_e value was closer to the Q_e value calculated from the linear plot. This suggests that the experimental data fit the pseudo-second-order model better than the pseudo-first-order model.

SEM analysis

SEM was used to identify the morphology of the surface of the *T. arjuna* bark powder before and after biosorption. The SEM micrographs of the adsorbent before adsorption showed them to be very porous and smooth (Figure 4(a)). Because of its porous structure, it could be concluded that the surface of the biosorbent has an adequate morphology for metal adsorption. There was a significant difference in the adsorbent surface after adsorption of metal which appeared rough (Figure 4(b)), implying interaction of the metal with the biomass surface. In addition to this, irregular and rough surfaces are found in metal adsorbed, due to which mass transfer resistance decreases, facilitating the diffusion of metal ions and enhancing the adsorption capacity.

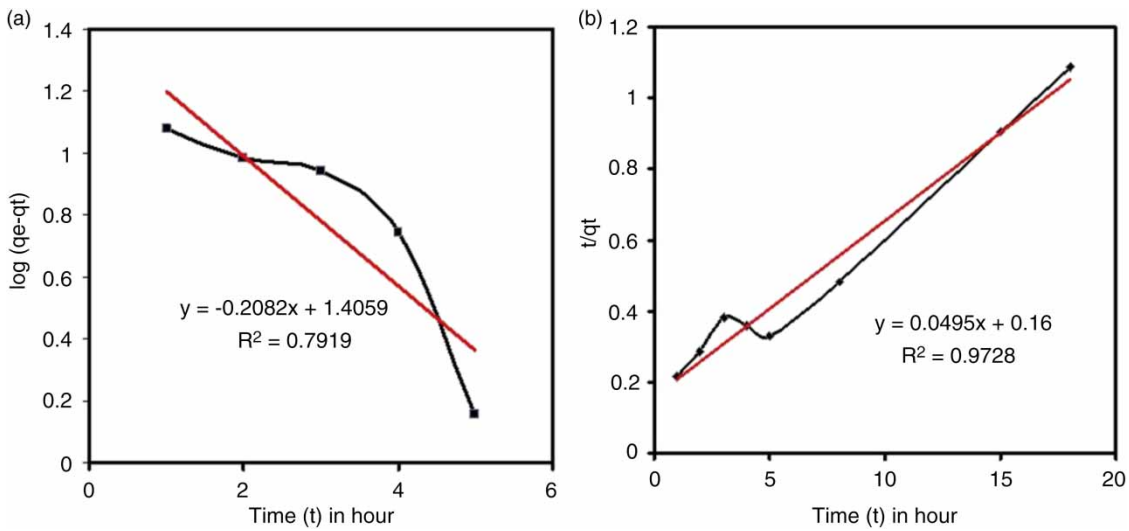

Figure 3 | Absorption kinetics: (a) pseudo-first-order kinetic model; (b) pseudo-second-order kinetic model.

Table 2 | The adsorption kinetics model parameters for Pr(III) adsorption on *T. arujuna* bark powder

C_i (ppm)	C_e (mg/L)	Q_e (mg/g)	Pseudo-first-order model			Pseudo-second-order model		
			K_1 (h^{-1})	Q_e (calculated value, mg/g)	R^2	K_2 (g mg^{-1} h^{-1})	Q_e (calculated value, mg/g)	R^2
80	5.43	16.6	0.48	25.47	0.7919	0.015	20.4	0.9728

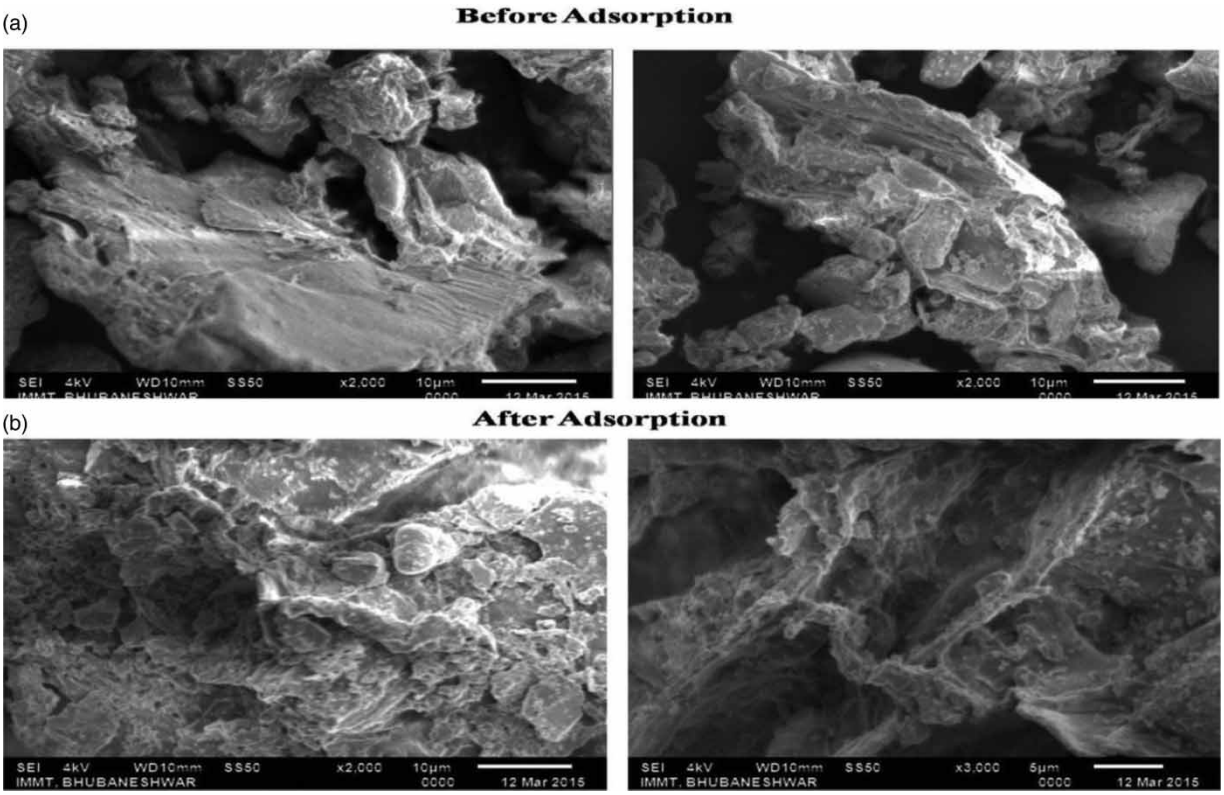

Figure 4 | SEM analysis of *Terminalia arjuna* plant bark powder: (a) before adsorption; (b) after adsorption.

EDAX analysis of biosorbent

The EDAX analysis was done in order to analyze the surface changes of the elements. The EDAX study of both raw biomass and metal-adsorbed biosorbent was performed in this experiment. Before adsorption the EDAX spectrum showed the presence of carbon (C), oxygen (O), calcium (Ca), and copper (Cu) (Figure 5(a)). The Cu peaks were due to the copper grid. The peaks of the other elements arose because of X-ray emissions from the proteins and chitins present in the cell wall of *T. arjuna* bark. After adsorption, several peaks of Pr(III) were found along with C, O, Ca, and Cu Peaks (Figure 5(b)). The presence of a strong Ca peak highlighted its role in the stabilization of structural components and it is these components that accounted for adsorption.

FT-IR analysis

The presence of functional groups in the raw biomass and metal-chelated biomass was revealed by the FT-IR analysis spectra. Figure 6(a) shows the results for raw biomass before adsorption. Figure 6(b) shows the metal-chelated biomass after adsorption. The peak at 3434.64 cm^{-1} represents the N-H stretching vibration in primary amine groups. The absorption bands at 3338.39 cm^{-1} and 3059.46 cm^{-1} were due to the O-H stretching frequency in aliphatic or aromatic hydroxyl groups. As there was intermolecular hydrogen bonding, this part of the region was very broad and more intense. A peak observed at 2943.57 cm^{-1} was due to the C-H stretching in alkanes. The peak located at 1620.66 cm^{-1} could be assigned to C = O stretching or amide bending. The presence of peaks in the 1,615–1,400 cm^{-1} range (1,550 cm^{-1} and

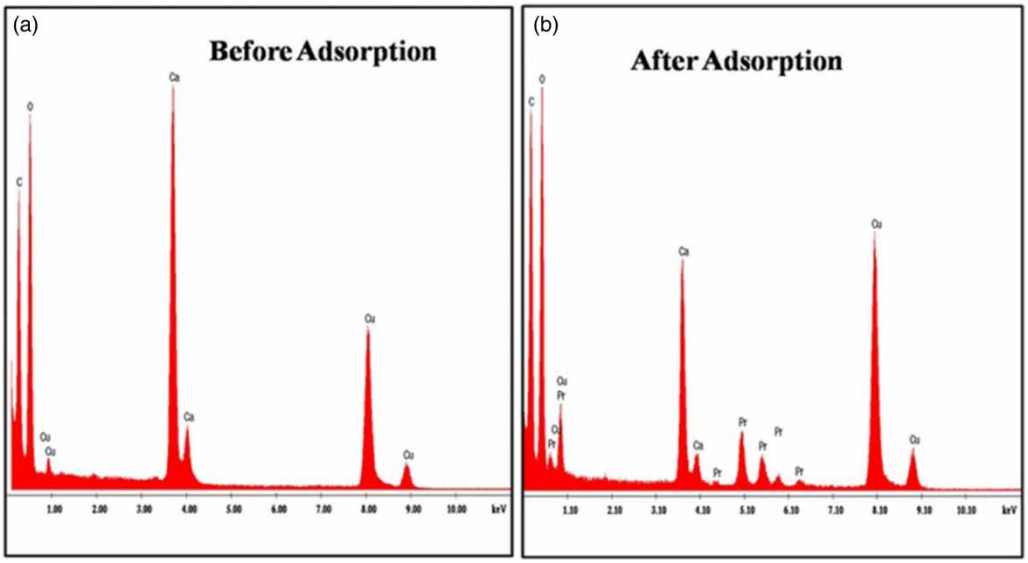

Figure 5 | EDAX analysis of *T. arjuna* bark powder: (a) before adsorption; (b) after adsorption.

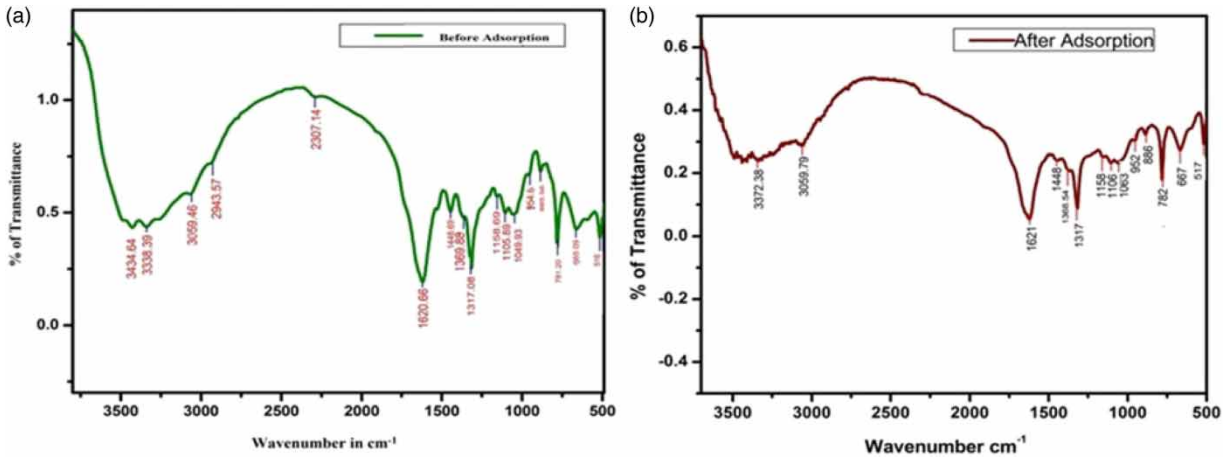

Figure 6 | FTIR spectrum of *T. arjuna* bark powder: (a) before adsorption; (b) after adsorption.

1448.69 cm^{-1}) were due to the C-C stretch in aromatic rings in the biomass. The peak at 1369.88 cm^{-1} was assigned to nitro N-O bending and a peak at 1105.89 cm^{-1} to C-O-C stretching in aromatic rings. The peaks that were observed at 1049.93 cm^{-1} showed the existence of the C-O bond in $-OCH_3$ groups. The peaks at 781.2 cm^{-1} and 516 cm^{-1} might have been due to halide groups. After adsorption the intensity of the absorption peaks was lower and slightly broader than the absorption band of the original raw biomass. After adsorption, the peaks at 3338.39 cm^{-1} (amine group), 1620.66 cm^{-1} (phenolic group), 1369.88 cm^{-1} (ester), 1049.93 cm^{-1}, 885.56 cm^{-1}, and 665.09 cm^{-1} (primary alcoholic groups) had shifted towards 3372.38 cm^{-1}, 1620.59 cm^{-1}, 1368.54 cm^{-1}, 1063.00 cm^{-1}, 886 cm^{-1}, and 667 cm^{-1}, respectively. This might have been due to the blockage of some functional groups by the metal at the time of adsorption. The Pr(III) metal ions were attaching to the surface of the biomass and some bonds were created between the metal and the functional groups of the biomass as shown by the decrease in intensity and shift of absorption peaks (Wahab *et al.* 2010).

MECHANISM OF METAL BINDING

From FT-IR analysis it was confirmed that the biomolecules of *T. arjuna* bark were involved in metal binding. Mainly

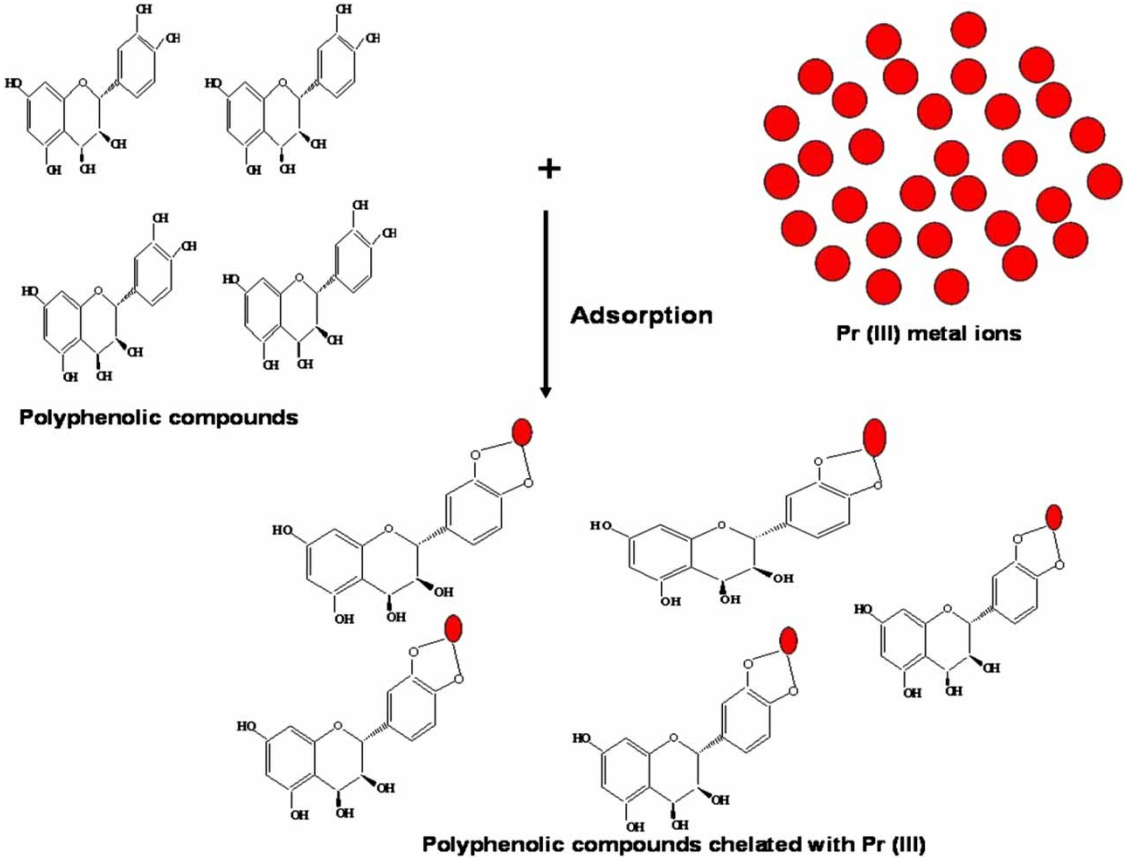

Figure 7 | Mechanism of binding of Pr(III) with polyphenolic compounds of *T. arjuna* bark.

the polar polyphenolic compounds present in the bark took part in metal binding due to the presence of a number of hydroxyl groups (Rakhi & Gopal 2012). The adjacent hydroxyl groups of the polyphenolic compounds chelated with Pr(III) metal ions. The mechanism of chelation of Pr(III) metal ion with the hydrous oxide surfaces of the polyphenolic compounds involves an ion exchange process in which the sorbed cations replace bound protons as shown in Figure 7.

REGENERATION STUDIES

The reusability of the biosorbent was tested several times by alternating adsorption and desorption cycles. Figure 8 shows the comparison of the percentage removal of Pr(III) using fresh and regenerated bark. The regenerated bark powder was reused for the adsorption of Pr(III) using the same initial metal concentration, which ranged between 20 and 80 ppm, as used for fresh bark powder. The percentage removal of Pr(III) was found to decrease from 91.92% to 89.9% in the third cycle when the metal concentration

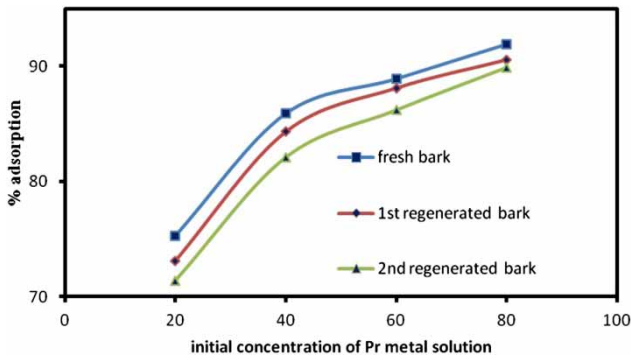

Figure 8 | Comparison for the % adsorption of Pr(III) using fresh and regenerated *T. arjuna* bark powder.

was 80 ppm. The above results suggest that the biosorbent could be effectively used for up to three cycles.

CONCLUSIONS

The present study showed that powdered bark of *T. arjuna* could be used as a promising adsorbent for the removal of

Pr(III) ions from water, i.e. 94% at pH 6.63. The process variables, such as pH, metal concentration, adsorbent dosage and contact time, played an important role in the adsorption process. Adsorption isotherm studies showed that the sorption data were well fitted to the Langmuir isotherm model with maximum capacity being 1.225 mg/g. From the Dubinin–Radushkevich model and the Temkin model, it was confirmed that the sorption of Pr is a physiosorption process. Furthermore, the adsorption process is spontaneous and follows pseudo-second-order kinetics. Regeneration studies showed that the bark powder of *T. arjuna* can be recovered for reuse, and high desorption efficiencies can be obtained over three adsorption-desorption cycles. It is a simple, green and economical biological procedure for the removal of Pr(III) ions from an aqueous environment using *T. arjuna* bark powder, and could prove to be an efficient alternative for the large-scale recycling of solutions to recover Pr contained in the waste.

ACKNOWLEDGEMENT

The authors thank Director, CSIR-IMMT, Bhubaneswar for providing the facilities to carry out this work and CSIR for funding the project.

CONFLICT OF INTEREST

The authors declare that they do not have any conflict of interest.

REFERENCES

Anastopoulos, I., Massas, I. & Ehaliotis, C. 2013 Composting improves biosorption of Pb^{2+} and Ni^{2+} by renewable lignocellulosic materials. Characteristics and mechanisms involved. *Chemical Engineering Journal* **231**, 245–254.

Anastopoulos, I., Bhatnagarb, A. & Limac, E. C. 2016 Adsorption of rare earth metals: a review of recent literature. *Journal of Molecular Liquids* **221**, 954–962.

Awwad, N. S., Gad, H. M., Ahmad, M. I. & Aly, H. F. 2010 Sorption of lanthanum and erbium from aqueous solution by activated carbon prepared from rice husk. *Colloids Surf. B.* **81** (2), 593–599.

Dabrowski, A. 2001 Adsorption- from theory to practice. *Adv. Colloid Interface Sci.* **93** (1–3), 135–224.

Dada, A. O., Olalekan, A. P., Olatunya, A. M. & Dada, O. 2012 Langmuir, Freundlich, Temkin and Dubinin–Radushkevich isotherms studies of equilibrium sorption of Zn^{2+} unto phosphoric acid modified rice husk. *Journal of Applied Chemistry* **3**, 38–45.

Das, N. & Das, D. 2013 Recovery of rare earth metals through biosorption: an overview. *Journal of Rare Earths* **31** (10), 933–943.

Das, D., Varsihini, J. S. & Das, N. 2014 Recovery of lanthanum(III) from aqueous solution using biosorbents of plant and animal origin: batch and column studies. *Mineral Engineering* **69**, 40–56.

Dubinin, M. M. & Radushkevich, L. V. 1947 The equation of the characteristic curve of activated charcoal. *Proc. Acad. Sci. USSR Phys., Chem. Sect.* **55**, 331–337.

Esposito, A., Pagnanelli, F., Lodi, A., Solisio, C. & Veglio, F. 2001 Biosorption of heavy metals by *Sphaerotilus natans*; an equilibrium study at different pH and biomass concentrations. *Hydrometallurgy* **60** (2), 129–141.

Foo, K. Y. & Hammed, B. H. 2010 Review: insight into the modeling of adsorption isotherms systems. *Chem. Eng. J.* **156** (1), 2–10.

Gardea-Torresdey, J. L., Tiemann, K. J., Peralta-Videa, J. G. & Parsons, M. 2004 Binding of erbium(III) and holmium(III) to native and chemically modified alfalfa biomass: a spectroscopic investigation. *Microchemical Journal* **76** (1–2), 65–76.

Kazy, S. K., Das, S. K. & Sar, P. 2006 Lanthanum biosorption by a *Pseudomonas* sp.: equilibrium studies and chemical characterization. *J. Ind. Microbiol. Biotechnol.* **33** (9), 773–783.

Kütahyali, C., Sert, S., Cetinkaya, B., Inan, S. & Eral, M. 2010 Factors affecting lanthanum and cerium biosorption on *Pinus brutia* leaf powder. *Sep. Sci. Technol.* **45** (10), 1456–1462.

Langergren, S. & Svenska, B. K. 1898 Zur theorie der sogenannten adsorption geloester stoffe. *K. Sven. Vetenskapsakad. Handl* **24** (4), 1–39.

Langmuir, I. 1916 The constitution and fundamental properties of solids and liquids. *J. Am. Chem. Soc* **38** (11), 2221–2295.

Nema, R., Jain, P., Khare, S., Pradhan, A., Gupta, A. & Singh, D. 2012 Preliminary phytochemical evaluation and flavanoids quantification of *Terminalia arjuna* leaves extract. *Int. J. Pharm. Phytopharmacol. Res* **1** (5), 283–286.

Oliveira, R. C., Jouannin, C., Guibal, E. & Garcia Jr, O. 2011 Samarium(III) and praseodymium(III) biosorption on *Sargassum* sp.: batch study. *Process Biochem* **46** (3), 736–744.

Philip, L., Iyengar, L. & Venkobachar, C. 2000 Biosorption of U, La, Pr, Nd, Eu, Dy by Pseudomonas aeruginosa. *Journal of Industrial Microbiology and Biotechnology* **25**, 1–7.

Qing, C. 2010 Study on the adsorption of lanthanum (III) from aqueous solution by bamboo charcoal. *J. Rare Earths* **28**, 125–131.

Rakhi, M. & Gopal, B. B. 2012 *Terminalia arjuna* bark extract mediated size controlled synthesis of polyshaped gold nanoparticles and its application in catalysis. *Int. J. Res. Chem. Environ.* 2 (4), 338–344.

Soylak, M. & Murat, I. 2014 A new coprecipitation methodology with lutetium hydroxide for preconcentration of heavy metal ions in herbal plant samples. *Journal of AOAC International* **97** (4), 1189–1194.

Takahashi, Y., Kondo, K., Miyaji, A., Watanabe, Y., Fan, Q., Honma, T. & Tanaka, K. 2014 Recovery and separation of rare earth elements using salmon milt. *PLoS ONE* **9** (12). doi:10.1371/journal.pone.0114858.

Temkin, M. I. & Pyzhev, V. 1940 Kinetics of ammonia synthesis on promoted iron catalyst. *Acta Phys. Chim. USSR* **12**, 327–356.

Varsihini, J. S., Das, D. & Das, N. 2014 Optimization of parameters for cerium(III) biosorption onto biowaste materials of animal and plant origin using 5-level Box-Behnken design: Equilibrium, kinetic, thermodynamic and regeneration studies. *Journal of Rare Earths* **32**, 745–758.

Vijayaraghavan, K. 2015 Biosorption of lanthanide (praseodymium) using *Ulva lactuca*: mechanistic study and application of two, three, four and five parameter isotherm models. *Journal of Environment and Biotechnology Research* **1** (1), 10–17.

Vijayaraghavan, K., Sathishkumar, M. & Balasubramanian, R. 2010 Biosorption of lanthanum, cerium, europium, and ytterbium by a brown marine alga, *Turbinaria conoides*. *Ind. Eng. Chem. Res* **49** (9), 4405–4411.

Wahab, M. A., Jellali, S. & Jedidi, N. 2010 Ammonium biosorption onto sawdust: FTIR analysis, kinetics and adsorption isotherms modeling. *Bioresource Technology* **101**, 5070–5075.

Xu, S., Zhang, S., Chen, K., Han, J., Liu, H. & Wu, K. 2011 Biosorption of $La^{3+}$and Ce^{3+} by *Agrobacterium* sp. HN1. *Journal of Rare Earths* **29** (3), 265–270.

Zhang, Z., Wang, Z., Chen, D., Miao, R., Zhu, Q., Zhang, X., Zhou, L. & Li, Z. 2014 Purification of praseodymium to $4N^{5+}$ purity. *Vacuum* **102**, 67–71.

Zhu, Y., Zheng, Y. & Wang, A. 2015 A simple approach to fabricate granular adsorbent for adsorption of rare elements. *Int. J. Bio. Macromolecules* **72**, 410–420.

First received 6 June 2017; accepted in revised form 7 November 2017. Available online 20 November 2017